Development 134, 1191-1201 (2007) doi:10.1242/dev.02804

Head regeneration in wild-type hydra requires de novo neurogenesis

Marijana Miljkovic-Licina*, Simona Chera, Luiza Ghila and Brigitte Galliot†

Because head regeneration occurs in nerve-free hydra mutants, neurogenesis was regarded as dispensable for this process. Here, in wild-type hydra, we tested the function of the ParaHox *gsx* homolog gene, *cnox-2*, which is a specific marker for bipotent neuronal progenitors, expressed in cycling interstitial cells that give rise to apical neurons and gastric nematoblasts (i.e. sensory mechanoreceptor precursors). *cnox-2* RNAi silencing leads to a dramatic downregulation of *hyZic*, *prdl-a*, *gsc* and *cnASH*, whereas *hyCOUP-TF* is upregulated. *cnox-2* indeed acts as an upstream regulator of the neuronal and nematocyte differentiation pathways, as *cnox-2*(–) hydra display a drastic reduction in apical neurons and gastric nematoblasts, a disorganized apical nervous system and a decreased body size. During head regeneration, the locally restricted de novo neurogenesis that precedes head formation is *cnox-2* dependent: *cnox-2* expression is induced in neuronal precursors and differentiating neurons that appear in the regenerating tip; *cnox-2* RNAi silencing reduces this de novo neurogenesis and delays head formation. Similarly, the disappearance of *cnox-2*$^+$ cells in *sf-1* mutants also correlates with head regeneration blockade. Hence in wild-type hydra, head regeneration requires the *cnox-2* neurogenic function. When neurogenesis is missing, an alternative, slower and less efficient, head developmental program is possibly activated.

KEY WORDS: Cnidarian, Evolution, Apical patterning, Regeneration, Neurogenesis, Neuronal progenitors, Interstitial stem cells, RNA interference, ParaHox gene, β-Tubulin

INTRODUCTION

Hydra belongs to Cnidaria, a phylum that arose before bilaterians and provides model systems to trace back ancestral developmental processes, as such as apical and anterior patterning (Galliot and Miller, 2000), neuromuscular differentiation (Miljkovic-Licina et al., 2004; Seipel and Schmid, 2005) and regeneration (Holstein et al., 2003; Galliot et al., 2006). Hydra polyps display a radial symmetry with an apex or head, centered on a mouth opening surrounded by tentacles that catch and ingest prey, and a basal disk at the opposite extremity. Throughout the animal, the body wall consists of two cell layers, the ectoderm and the endoderm, separated by an extracellular matrix called mesoglea. These two cell layers are made up of myoepithelial cells and interstitial stem cells, which provide precursors for gland cells, neurons, nematocytes and germ cells.

The hydra nervous system is organized as a nerve net that extends throughout the animal and is made up of two cell lineages: the sensory mechanoreceptor cells, named nematocytes, and the neurons, with typical synapses (Westfall, 1996). Those two cell types follow distinct differentiation pathways (Bode, 1996). Nematoblasts undergo several synchronous divisions, forming syncitial cell clusters in the ectoderm of the body column, before differentiating a typical capsule, the nematocyst, and migrating toward the tentacles. By contrast, neuronal precursors follow a more direct differentiation pathway, responding to local cues along the body axis (Fujisawa, 1989). Moreover, differentiated neurons constantly change their phenotype as they get displaced toward the extremities (Bode, 1992). Thus, although hydra anatomy appears very simple, highly dynamic processes are required for its maintenance. Besides homeostasis, morphogenesis takes place in sexual and asexual contexts, such as budding, regeneration and reaggregation. Head regeneration, which leads to the replacement of the missing part after 2 days, relies on the setting up of an organizer activity at the regenerating tip (MacWilliams, 1983). This requires the sequential activation of a specific set of 'early' genes within the endodermal cells of the regenerating tip, followed 16-20 hours post-amputation (hpa) by the activation of the 'early-late' genes at the head patterning stage (Galliot et al., 2006), when an intense cell proliferation takes place in the regenerating tip (Holstein et al., 1991).

According to several independent datasets, neurons are thought to play a minor role in de novo head patterning: chimera experiments demonstrated the primary role of myoepithelial cells in budding rate and regenerative capacity, whereas nerve-free hydra display amazing budding and regenerative abilities (Fujisawa and Sugiyama, 1978; Marcum and Campbell, 1978). More recently the systematic screening of hydra peptides with morphogenetic function identified mostly epitheliopeptides (Fujisawa, 2003). However, neurons were also shown to produce morphogenetic peptides involved in head differentiation (Schaller et al., 1989; Javois and Frazier-Edwards, 1991) and interstitial cells (i-cells) can regulate the morphogenetic potential of the myoepithelial cells (Sugiyama and Wanek, 1993). Therefore, the interplay between interstitial and myoepithelial cells in homeostatic and developmental contexts appears essential but largely unknown.

In this work, we have investigated the putative role of neurogenesis in head regeneration by dissecting the cellular and developmental regulation of *cnox-2*, the hydra *gsx* homolog gene. Cnidarian *gsx/ind*-related genes were identified in numerous cnidarian species, and their expression patterns suggest an ancestral *gsx/cnox-2* function in neurogenesis and oral patterning. The *cnox-2/anthox2* genes are activated during apical patterning in hydra

Department of Zoology and Animal Biology, University of Geneva, Sciences III, 30 Quai Ernest Ansermet, CH-1211 Geneva 4, Switzerland.

*Present address: Department of Pathology and Immunology, University Medical Center, rue Michel Servet 1, CH-1211 Geneva 4, Switzerland
†Author for correspondence (e-mail: brigitte.galliot@zoo.unige.ch)

Accepted 10 January 2007

(Schummer et al., 1992; Gauchat et al., 2000), display an apical expression in the *Hydractinia* gastrozooid polyps (Cartwright et al., 1999) and the sea anemone *Nematostella* juvenile polyps (Finnerty et al., 2003). In the *Nematostella* planula larva, *anthox2* transcripts are localized at the posterior pole, which provides the future oral pole of the polyp. In the early *Podocoryne* larva, the *gsx* transcripts, initially localized in the anterior endoderm, extends toward the posterior pole (Yanze et al., 2001). However, in the coral *Acropora* developing larva, *cnox-2* expression was detected in neurons of the ectodermal central region of the body axis and rarely in the oral region (Hayward et al., 2001), suggesting some variability in the developmental but not the cellular regulation of the cnidarian *gsx/cnox-2* gene family. Nevertheless, in hydra, contradicting data were published as immunochemistry analyses showed a predominant cnox-2 expression in the myoepithelial cells of the body column and a repression during head formation (Shenk et al., 1993a; Shenk et al., 1993b). Therefore a *gsx/cnox-2* consensus function remains questionable in cnidarians (Schierwater et al., 2002). We show here that *cnox-2* expression in hydra is indeed restricted to the nervous system in both homeostatic and developmental contexts. By analysing the proliferation rate of *cnox-2*$^+$ cells, we identified a subpopulation of interstitial stem cells that behave as bipotent neuronal progenitors, giving rise to apical neurons and nematoblasts. Functional assays using RNAi in wild-type hydra indicate that those *cnox-2*$^+$ progenitors promote apical neurogenesis and head patterning during head regeneration.

MATERIALS AND METHODS

Culture of animals and regeneration experiments

Hydra vulgaris (*Hv*, Zürich, Basel, AEP strains), *Hydra magnipapillata* (*Hm-105*, *sf-1* strains) were cultured as in Gauchat et al. (Gauchat et al., 2004). *sf-1* mutants were kept for 2 days at 28°C to eliminate i-cells, and they were subsequently amputated and maintained at 28°C, whereas control *sf-1* hydra were kept at 18°C. Bisection was mid-gastric in all regeneration experiments.

Bromodeoxyuridine labeling coupled to whole-mount in situ hybridization

Intact hydra (*Hm*) were continuously incubated with bromodeoxyuridine (BrdU) 5 mmol/l (Sigma) for 2, 24 or 48 hours, immediately fixed, processed for *cnox-2* whole-mount in situ hybridization (WM-ISH) and detected for BrdU as in Gauchat et al. (Gauchat et al., 2004). For regeneration experiments, intact hydra were incubated for 4 hours in BrdU, washed, immediately bisected and left in Hydra medium. *cnox-2 Hv* cDNA was amplified using M13 forward-20 and reverse primers or restricted at the *Eco*RI site. *cnox-2* riboprobes were either DIG- or fluorescein-labeled. Imaging was performed on Axioplan2 and LSM 510 META confocal microscopes (Zeiss).

Double-labeling WM-ISH with tyramide detection

After hybridization to the mixed DIG-labeled *hyZic* and fluorescein-labeled *cnox-2* riboprobes, the samples were first incubated in the mouse anti-FITC antibody (1:100, Sigma) and detected with the TSA-Kit#2 (Alexa 488, Invitrogen or Molecular Probes). For the second probe a sheep anti-DIG antibody (1:400, Roche) was used, followed by the detection with an anti-sheep HRP (1:100, Sigma) and the TSA-Kit#41 (Alexa 555). The tyramide labeling time was 18 minutes. Samples were washed 3× 10 minutes in PBS, mounted in Mowiol and pictured either at the Zeiss Axioplan2 microscope using a FITC filter or at the Leica SP2 confocal.

Immunohistochemistry with tyramide detection

Standard immunohistochemistry was performed on either freshly fixed or in situ processed whole-mount animals. Samples were washed in PBS for 3× 10 minutes, treated with 3% H_2O_2/PBS for 1 hour, blocked in 2% BSA and incubated in the mouse monoclonal β-tubulin antibody (1:1500, Sigma clone 2-28-33) ON at 4°C. Subsequently the animals were washed for 3× 10 minutes in PBS and incubated in the anti-mouse HRP antibody (1:100) for 3 hours at room temperature. The samples were detected with the TSA-Kit#2 as above.

Double-stranded RNA interference

The *cnox-2 Hv* 795 bp PCR product amplified with the cx2-hv-Xmn5′ (GAACCTCTTCTTAAAACGAGTTAG) and the cx2-hv-16HB3 (GTAGGGGAATAGCTATATCCTTTCTTA) primers was inserted into the *Sma*I-digested double T7 vector pPD129.36 (L4440, Fire's laboratory). Double-stranded RNAs (dsRNAs) were produced in HT115(DE3) bacterial strain (Timmons and Fire, 1998). Fifty intact *Hv* hydra per condition starved for 2 days were given every other day up to nine times grinded agarose that contained either no bacteria, or bacteria having produced control dsRNAs (transformed with the L4440 vector) or dsRNAs corresponding to *cnox-2* or *Kazal1* (Chera et al., 2006). The day following the last dsRNA exposure, samples were processed for RT-PCR or WM-ISH, or bisected for regeneration experiments.

Semi-quantitative RT-PCR analysis

mRNA was prepared from intact hydra (*Hv* Basel) or upper halves collected immediately post-amputation with the QuickPrep micro-mRNA Purification Kit (Amersham) and resuspended in 10 μl H_2O. mRNA (50 ng) was used for Sensiscript Reverse Transcription (Qiagen) and specific cDNAs were PCR amplified for up to 24 cycles with gene-specific primers (sequences on request).

RESULTS

cnox-2 is expressed in the neuronal and mechanoreceptor cell lineages

In three hydra species (*Hv*, *Hm-105*, *Hvi*), *cnox-2* expressing cells were detected in the ectodermal layer of the adult polyp, in two distinct regions: first in the apex, at the level of the tentacle zone and immediately above; second along the body column but absent from the peduncle and basal disk (Fig. 1A-C,G,H, not shown). Beside single i-cells and pairs of dividing i-cells expressing *cnox-2* in both regions, *cnox-2*$^+$ cell types were not identical in these two locations. In the apex, *cnox-2*$^+$ cells also displayed a typical neuronal shape, mostly multipolar neurons as evidenced by the β-tubulin co-staining (Fig. 1B,D, and see Fig. S1A-E in the supplementary material), whereas in body column, *cnox-2*$^+$ cells formed clusters, typical of synchronously dividing nematoblasts (Fig. 1C,E). Quantitative analysis of these clusters (Fig. 1F) showed that *cnox-2* is expressed at earliest stages of nematoblast proliferation, being detected in pairs of i-cells (20%) and four- and eight-cell clusters (80%), but rarely in 16-cell clusters (<1.3%). Moreover, nematoblasts differentiating a typical capsule never expressed *cnox-2* (Fig. 1C, asterisks), implying that *cnox-2* expression ceases when nematoblasts differentiate.

To verify that *cnox-2* expression was restricted to i-cell lineages, we tested the *sf-1* mutants that lose their i-cells after a 2 day temperature shift but maintain their myoepithelial cells intact (Marcum et al., 1980). At permissive temperature, *cnox-2* expression was as in wild type (Fig. 1G,H), whereas at restrictive temperature *cnox-2* expression was abolished (Fig. 1I,J), confirming that *cnox-2* expression is absent from the myoepithelial cell lineages. In addition, in wild-type hydra, none of the other i-cell derivatives, including gland cells (not shown), testes and ovaries (Fig. 1K-N) expressed *cnox-2*. In female hydra, the region facing the ovary was *cnox-2* negative (Fig. 1K,L), probably because of the recruitment of i-cells as nurse cells by the mature oocyte. Therefore *cnox-2* expression appears restricted to two cell lineages among the i-cells: neuronal at the apical pole and mechanoreceptor along the body column.

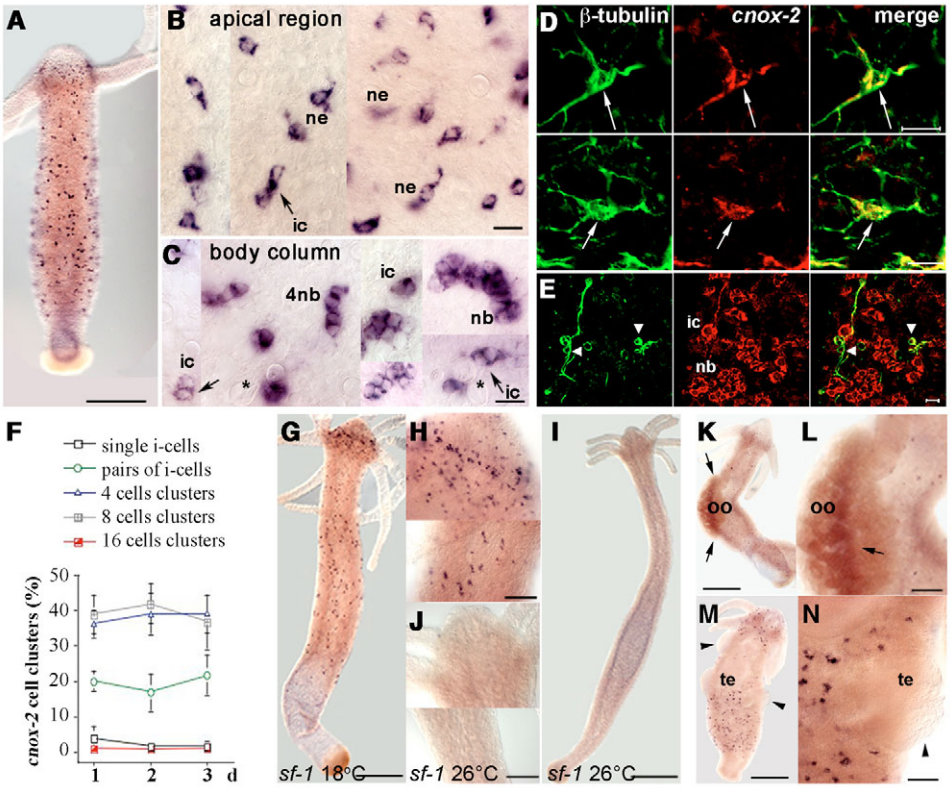

Fig. 1. *cnox-2* expression in the interstitial cell, mechanoreceptor and neuronal cell lineages. (**A**) *cnox-2* expression in adult polyps of *Hv*. (**B**) Apical *cnox-2*$^+$ pairs of dividing i-cells (arrow) and differentiated neurons. (**C**) Gastric *cnox-2*$^+$ i-cells, either single or twins, and clusters of synchronously dividing nematoblasts. (**D**) *cnox-2*$^+$ apical multipolar neurons (arrows) detected with anti-β-tubulin staining (see Fig. S1 in the supplementary material). (**E**) *cnox-2*$^+$ gastric cells that correspond to i-cells and nematoblast clusters but not neurons (arrowheads). D and E are confocal views. (**F**) Distribution of the i-cells and nematoblast clusters among the gastric *cnox-2*$^+$ cells during starvation counted on ten hydra. (**G-J**) *cnox-2* expression in the *sf-1* mutant maintained at permissive (18°C, G,H) or restrictive (26°C, I,J) temperatures for 2 days. (**K-N**) Absence of *cnox-2* expression during oogenesis (K,L, arrows) and spermatogenesis (M,N, arrowheads). Scale bars: 400 μm in A,G,I,K,M; 100 μm in H,J,L,N; 20 μm in B,C; 10 μm in D,E. ic, i-cell; nb, nematoblast; ne, neuron; oo, oocyte; te, testes.

cnox-2$^+$ i-cells are cycling cells

Single or twin i-cells form a heterogeneous cell population that includes self-renewing stem cells and precursors to a variety of cell types including gametes, gland cells, neuronal cells and nematoblasts (Holstein and David, 1990a). As *cnox-2* transcripts were detected neither in gland cells nor in gametes, the *cnox-2*$^+$ i-cells may represent three distinct populations: self-renewing interstitial stem cells, neuronal precursors and nematoblast precursors. The cycling activity of *cnox-2*$^+$ cells was measured through continuous BrdU-labeling (Fig. 2): in body column over 90% *cnox-2*$^+$ cells were BrdU-positive after 2 hours (Fig. 2A,D,G), reaching 100% after 24 hours (Fig. 2B,E,G). Given that S-phase lasts about 12 hours in all i-cells (Campbell and David, 1974) and that a 15 minute incubation is sufficient to detect BrdU-incorporation (data not shown), we calculated that the gastric *cnox-2*$^+$ cells would traverse the cell cycle in about 16 hours if cells are not synchronized.

In the apex, a significant number of *cnox-2*$^+$ cells were BrdU-labeled: about 4, 23 and 45% after 2, 24 and 48 hours, respectively (Fig. 2D-F,H). After 24 and 48 hours' incubation, some of those BrdU$^+$/*cnox-2*$^+$ cells corresponded to newly differentiated neurons. In fact, pairs of apical BrdU$^+$/*cnox-2*$^+$ cells were often observed, showing extended processes, corresponding to precursors that differentiate into *cnox-2* neurons immediately after mitosis (Fig. 2E). Thus *cnox-2*$^+$ i-cells correspond to a subset of cycling i-cells that provide apical neurons and proliferating nematoblasts and can therefore be regarded as bipotent neuronal progenitors.

Starvation affects *cnox-2* expression in the body column but not in the apex

Hydra starvation leads to dramatic cellular rearrangements in both epithelial (Bosch and David, 1984; Holstein et al., 1991) and interstitial (Gauchat et al., 2004) cell compartments. In case of *cnox-2*$^+$ cell clusters, their distribution was not significantly affected over the first 3 days, except for a slight decrease in the single i-cell compartment (Fig. 1G). However, when starvation was prolonged over 10 days, a drastic reduction in the number of gastric *cnox-2*$^+$ cells was recorded (Fig. 3G), whereas the number of apical *cnox-2*$^+$ cells did not vary (Fig. 3F). Hence starvation drastically alters the production and/or survival of *cnox-2*$^+$ nematoblasts, but not of the apical *cnox-2*$^+$ lineage.

Efficient *cnox-2* downregulation through RNAi

We next tested *cnox-2* function through RNAi loss-of-function assay. *Kazal1* was selected as control gene, as its expression is restricted to a distinct i-cell lineage, the gland cells (Chera et al., 2006). Moreover, *cnox-2* and *Kazal1* did not show any epistatic relationships, as evidenced by their conserved respective expressions in *Kazal1*(–) and *cnox-2*(–) hydra (Fig. 3B, Fig. 4A,B). *cnox-2* silencing was effective and specific, as shown by RT-PCR and WM-ISH assays: hydra exposed repeatedly to *cnox-2* dsRNAs exhibited a drastic reduction in *cnox-2* transcripts levels, whereas *actin*, *Kazal1* and *CREB* levels remained unaffected (Fig. 3A, Fig. 4B). When whole hydra were compared to upper halves (enriched in apical tissue), *cnox-2* silencing appeared stronger in the former ones, even though the control level of *cnox-2* expression was significantly lower in whole hydra than in apically enriched tissue (Fig. 3A, lanes 1,3). Therefore, the decrease in *cnox-2* levels in the body column probably corresponded to the addition of two distinct effects: the specific *cnox-2* RNAi knockdown and the starvation effect described above, leading to a drastic decrease in nematoblast production. WM-ISH confirmed the progressive disappearance of *cnox-2*$^+$ cells with the successive dsRNA exposures, becoming very rare after five feedings in gastric (Fig. 3C) and apical (Fig. 3D,E) regions. The number of *cnox-2*$^+$ apical cells was significantly reduced after five exposures, by 55 and 38% when compared to mock-silenced and *Kazal1*(–) hydra, respectively (Fig. 3F). In body column, a single dsRNA exposure led to a 48% decrease in *cnox-2*$^+$ cell number (Fig. 3G, lanes 1-3). However,

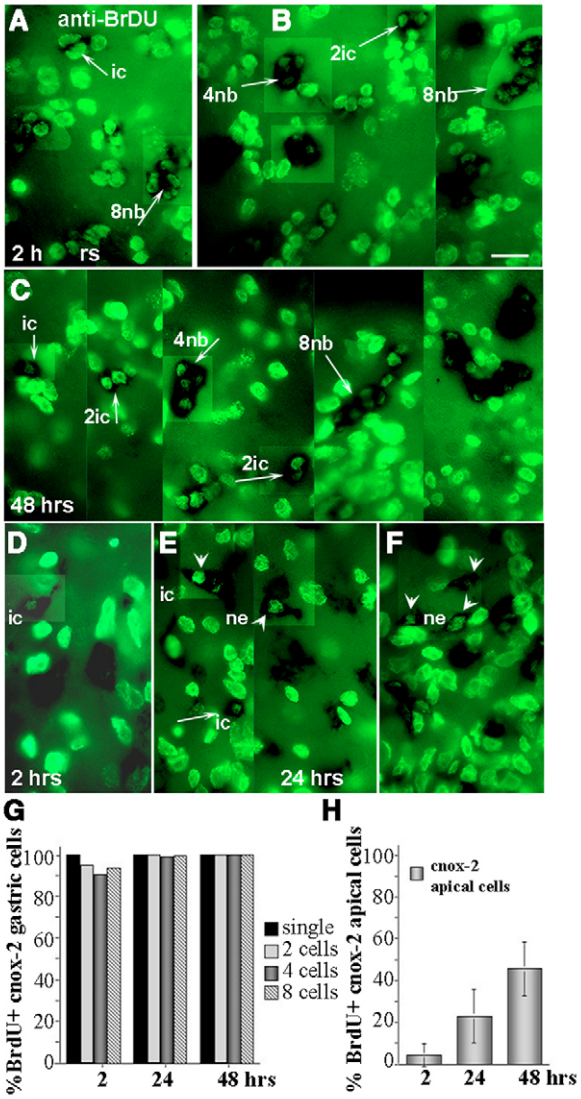

Fig. 2. *cnox-2*$^+$ cells are cycling cells in intact hydra. (**A-F**) *cnox-2*$^+$ (dark blue) and BrdU-labeled (green) cells detected in the body column (A-C) and the apex (D-F) after 2 (A,D), 24 (B,E) or 48 hours (C,F) continuous BrdU incubation. Arrows indicate i-cells and nematoblasts, arrowheads neurons. (**G**,**H**) Percentage of gastric (G) and apical (H) BrdU$^+$/*cnox-2*$^+$ cells (n=10). Scale bar: 40 μm. ic, single i-cell; 2ic, pairs of i-cells; nb, nematoblast; ne, neuron.

after five exposures, the 12 day starvation effect was dramatic, and the difference between control and *cnox-2* RNAi hydra was no longer significant (Fig. 3G, lanes 4-6). This loss of function obviously affected hydra homeostasis, as *cnox-2*(–) hydra progressively became significantly smaller than *Kazal1*(–) or control hydra (Fig. 3B,C): about twice as short as control hydra after nine exposures (hydra exposed 9× to *cnox-2* dsRNAs: 0.44 mm ± 0.18; to control dsRNAs: 0.85 mm ± 0.28, n=10).

Disorganization of the apical nervous system in *cnox-2*(–) adult polyps

To detect whether the decrease in *cnox-2*$^+$ apical expression affected the organization of the apical nervous system (ANS) (Fig. 3H-M), we used the anti-β-tubulin antibody (Siddiqui et al., 1989) that stains all types of neurons, nematocytes and some i-cells, but not nematoblasts or myoepithelial cells (Fig. 1D,E, and see Fig. S1G,H in the supplementary material). This staining showed a highly organized ANS, with parallel processes of the sensory neurons along the hypostome (the domed region from the mouth opening down to the tentacle zone) providing an inverted-basket aspect (Fig. 3H,I, arrows, and see Fig. S2 and Movie S1 in the supplementary material). On sagittal views, the multipolar neurons were visible, spread along meridian lines that converge toward the mouth opening (Fig. 3H). After five *cnox-2* dsRNA exposures, the ANS was dramatically reduced, restricted to its most apical part, whereas the sub-tentacle zone became nerve-free. The density of sensory neurons was decreased, the systematic parallel orientation of their processes was altered and their connections to the multipolar neurons were no longer visible (Fig. 3J,L, and see Fig. S2 in the supplementary material). After nine exposures, apical neurons were no longer detected (Fig. 3N), indicating that *cnox-2* expression is required to maintain apical neurogenesis and ANS organization.

cnox-2 is an upstream regulatory gene in the nematocyte differentiation pathway

Previous cellular expression analyses identified several candidate genes as regulators of the nematocyte differentiation pathway. Those genes display cellular expression patterns with striking differences when considering the proliferation rate, the cluster size and the presence of a differentiating capsule. *cnox-2* is expressed in precursors and at early proliferative stages but is repressed as soon as nematoblasts differentiate (this work); *hyZic* is also expressed at early stages (Lindgens et al., 2004), but with a lower representation among precursors (6% for *hyZic*, over 20% for *cnox-2*) and a lower BrdU-labeling index after a short incubation than *cnox-2* (40 versus 95%). Therefore, *hyZic* is probably turned on at a slightly later stage than *cnox-2* and appears to be a candidate *cnox-2* target gene. As additional regulators, the *hyCOUP-TF* orphan receptor was proposed to repress proliferation in nematoblast clusters, switching them to differentiation (Gauchat et al., 2004), whereas the achaete-scute homolog *CnASH* is expressed in non-proliferative differentiating nematocytes (Lindgens et al., 2004). Finally, the transcription factor CREB is expressed at all proliferative stages of this pathway (Chera et al., 2007).

Cellular expression analysis showed that *cnox-2* and *hyZic* transcripts indeed colocalize in most i-cells and nematoblast clusters (Fig. 4A). Moreover, in *cnox-2*(–) hydra, *hyZic* and *CnASH* transcripts were undetectable, *hyCOUP-TF* was upregulated and *CREB* was unaffected (Fig. 4B, left). These results support an upstream role for *cnox-2* (Fig. 4C).

cnox-2 regulates apical neurogenesis

As well as the nematocyte pathway, *hyCOUP-TF*, *CnASH* and *CREB* are also expressed in the neuronal lineage (Gauchat et al., 2004; Hayakawa et al., 2004; Chera et al., 2007), whereas other genes display a neuronal-specific expression, such as the PRD-class *prdl-a* (Gauchat et al., 1998) and *gsc* (Broun et al., 1999), the ANTP-class *msh* (Miljkovic-Licina et al., 2004) and the *RFamide* neuropeptide genes (Mitgutsch et al., 1999). Their RT-PCR expression analysis in *cnox-2*(–) and control hydra showed a significant downregulation of *prdl-a*, *gsc* and *RFamide-B*, whereas *hyCOUP-TF* was found to be upregulated (Fig. 4B, right), indicating that *cnox-2* contributes to the regulation of those neuronal apical genes. Moreover, *msh* expression in the gastric region was slightly decreased, suggesting that gastric *cnox-2*$^+$ i-cells also provide neuronal precursors in this region.

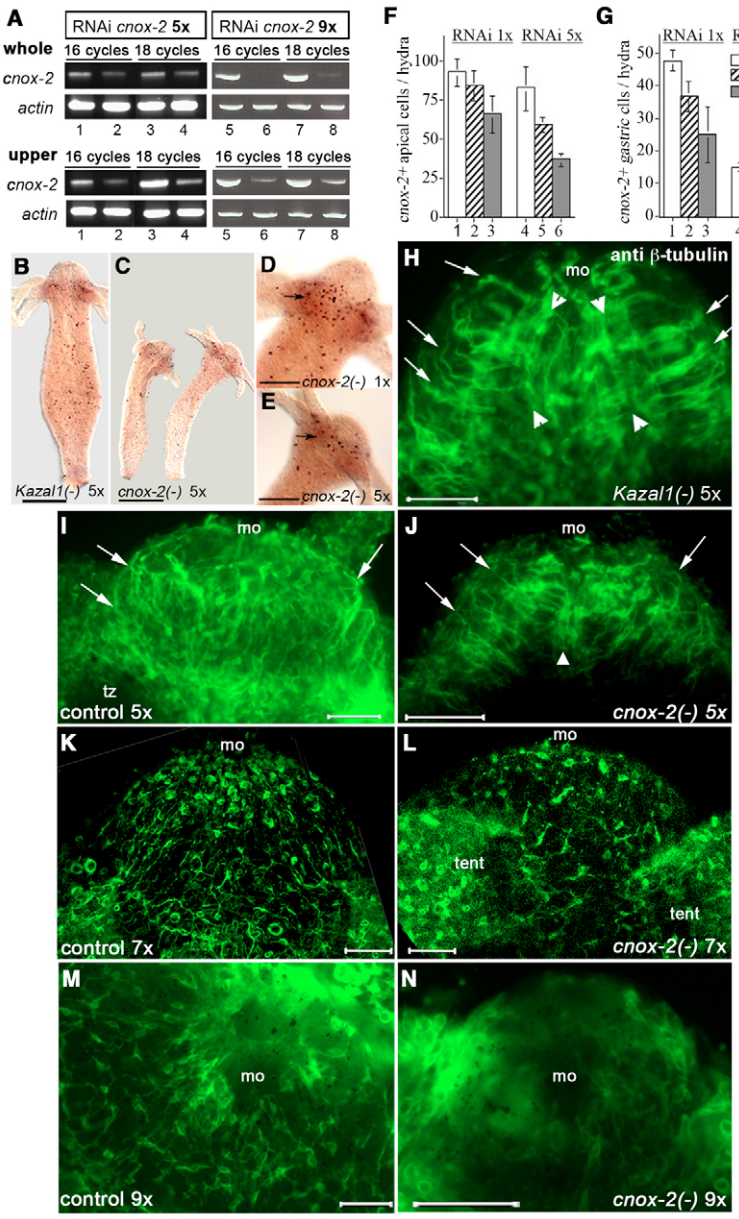

Fig. 3. Apical neurogenesis is altered in RNAi *cnox-2* knocked-down hydra. (**A**) RT-PCR assay showing *cnox-2* expression levels in whole polyps (upper panel) or upper halves collected immediately after bisection (lower panel), exposed 5× and 9× to control (lanes 1,3,5,7) or *cnox-2* (lanes 2,4,5,8) dsRNAs. (**B-E**) *cnox-2* expression pattern in hydra exposed to *Kazal1* (B) and *cnox-2* (C-E) dsRNAs. Note the reduced size of hydra in C. (**F**,**G**) Number of apical (F) and gastric (G) *cnox-2*$^+$ cells per hydra exposed once or 5× to control (lanes 1,4), *Kazal1* (lanes 2,5), *cnox-2* (lanes 3,6) dsRNAs. (**H-N**) Disorganization of the ANS upon *cnox-2* silencing detected by anti-β-tubulin staining (see Fig. S2 and Movie S1 in the supplementary material). (H,I,K,M) In control and *Kazal1(-)* hydra, the ANS formed of parallel sensory neurons (arrows) and meridien multipolar neurons (arrowheads) extends from the tentacle zone up to the mouth opening. (J,L) Reduced and disorganized ANS after 5× and 7× *cnox-2* dsRNAs exposures. (M,N) Apical neurons are no longer detected after 9× *cnox-2* dsRNA exposures. H,J,K,L: maximum projection confocal views; I,M,N: axioplan views. Scale bars: 400 μm in B,C; 200 μm in D,E; 50 μm in H-N. mo, mouth opening; tent, tentacules; tz, tentacle zone.

Concomittant de novo neurogenesis and *cnox-2* upregulation during apical patterning

De novo neurogenesis, restricted to head-regenerating tips and occurring at a time depending on the bisection level, early after decapitation and 'early-late' after gastric bisection, was previously reported (Venugopal and David, 1981). To monitor the cellular remodeling occurring in head-regenerating halves, we used the anti-β-tubulin staining and observed the complete disappearance of any neurons from head-regenerating tips for the first 16 hpa (Fig. 5A, and see Fig. S3 in the supplementary material). Thereafter, pairs of i-cells appeared (Fig. 5A, arrows), becoming more and more numerous, until a neuronal network was detected again when tentacle buds (TBs) emerged.

Interestingly, in head-regenerating tips, *cnox-2* displayed two opposite successive regulations that parallel the de novo neurogenesis described above. For the first 20 hpa, the head-regenerating tips were devoid of *cnox-2*$^+$ cells (Fig. 5B). Subsequently dividing *cnox-2*$^+$ i-cells first became visible (Fig. 5B,D, Fig. 6A), preceding the appearance of neuronal precursors and differentiated *cnox-2*$^+$ neurons (Fig. 5E,F, Fig. 6E), which gradually reached a maximum density at 48 hpa (Fig. 5J). This early-late *cnox-2* regulation, in agreement with the previously reported increase in *cnox-2* transcripts in the head-regenerating *H. viridissima* at 24 hpa (Schummer et al., 1992), was specific to the head-regeneration process, as it was not detected in foot-regenerating tips whatever the time point (Fig. 5B,C, arrowheads). By contrast, the *cnox-2*$^+$ neuronal density in the heads of foot-regenerating halves remained stable all through the regeneration process (Fig. 5C, right panel).

Along the body column a simultaneous decrease in the number of *cnox-2*$^+$ cells in both head- and foot-regenerating halves was observed at 24 and 36 hpa, lowered by 40-50% of the normal level in undisturbed polyps (Fig. 5C,H). This downregulation affected proliferating nematoblasts but not single i-cells, those actually showing a 2-fold increase of their density at 16 hpa (Fig. 5I). Therefore this reduction in gastric *cnox-2*$^+$ cells probably corresponds to the cell death of differentiating nematoblasts linked

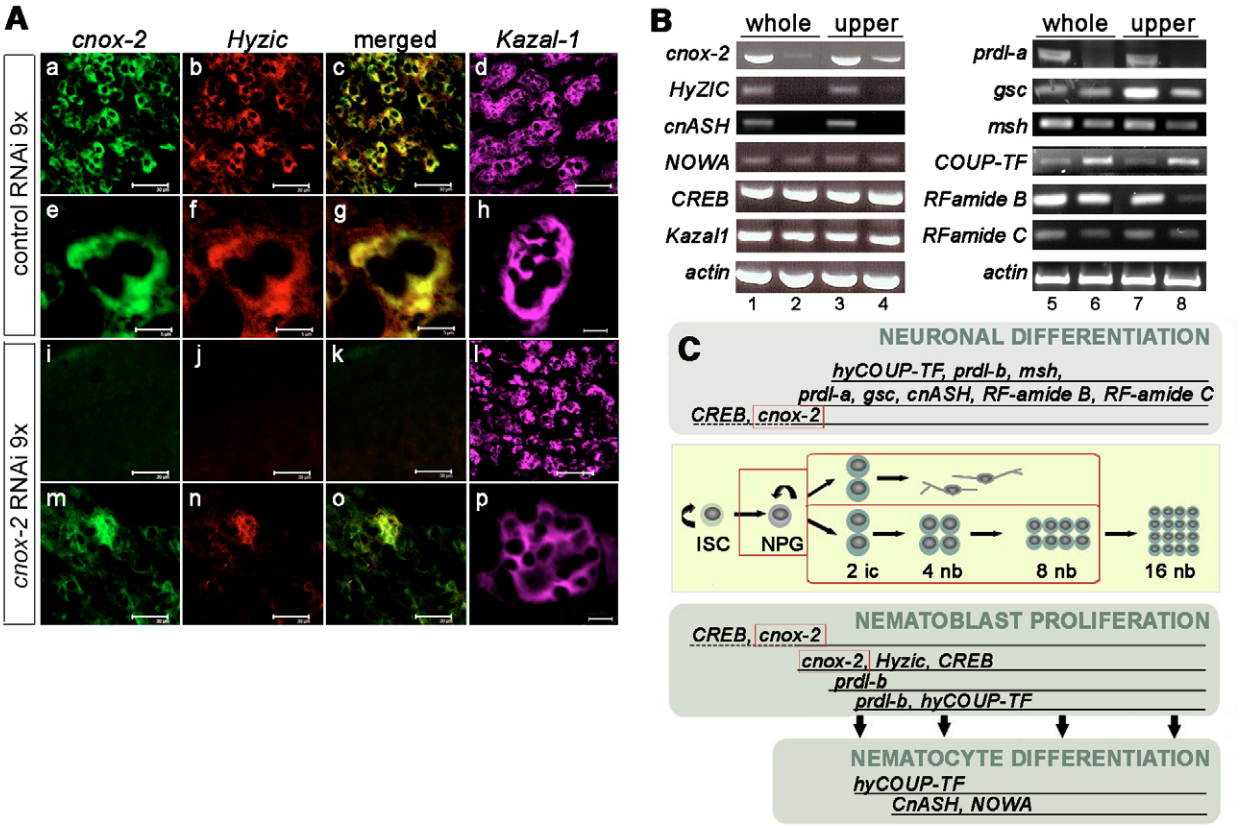

Fig. 4. *cnox-2* acts as an upstream regulator of the nematocyte and neuronal differentiation pathways. (**A**) Colocalization of the *cnox-2* (green) and *hyZic* (red) transcripts in nematoblast clusters (a-c) and dividing i-cells (e-g). After 9× *cnox-2* dsRNA exposures, expression of *cnox-2* and *hyZic* is either abolished (i-k, hydra1) or residual (m-o, hydra2). In *cnox-2*(–) hydra1, *Kazal1* expression in gland cells (purple, l,p) is similar to control (d,h). Scale bars: 30 μm in a-d,i-o; 5 μm in e-h,p. (**B**) Expression of genes expressed in the nematocyte (left) and/or neuronal (right) cell lineages of hydra exposed 5× to control (lanes 1,3,5,7) or *cnox-2* (lanes 2,4,6,8) dsRNAs. Number of cycles: 18 except *hyZic* (24), *msh* (16), *hyCOUP-TF* (16). (**C**) Scheme depicting the putative regulators of interstitial stem cells, neuronal progenitors, interstitial cells, neurons and nematoblasts. ic, interstitial cell; ISC, interstitial stem cell; nb, nematoblast; ne, neuron; NPG, neuronal progenitor.

to the amputation stress as previously reported (Fujisawa and David, 1984), a scenario supported by the transient relative increase in single *cnox-2*$^+$ i-cells.

During budding, numerous *cnox-2* cells were detected in the distal tip from stage 3 onward (Fig. 5G). This stage, which occurs 16-20 hours before TBs become visible (Otto and Campbell, 1977), corresponds to the onset of the early-late transition during regeneration. Similarly to head-regenerating tips, those *cnox-2*$^+$ cells were identified as dividing i-cells, neuronal precursors and differentiated neurons, first broadly distributed, becoming restricted to the tentacle zone and the basis of the hypostome at stage 7-8. Therefore, during budding and regeneration, *cnox-2* exhibits a similar spatiotemporal regulation in the presumptive head region; the initiation of its expression in the neuronal cell lineage precedes by 20 hours the emergence of the TBs. However, during budding, *cnox-2*$^+$ expression in the body column of the growing bud was not altered (Fig. 5G), indicating that the negative 'post-amputation' gastric regulation does not take place here.

De novo differentiation of *cnox-2* neurons in head-regenerating tips

To trace back the origin of the *cnox-2*$^+$ neurons detected in head-regeneration tips, hydra were BrdU-labeled for 4 hours before bisection and BrdU$^+$/*cnox-2*$^+$ cells were analysed during early-late regeneration (Fig. 6). From 20 to 44 hpa, the density of BrdU$^+$ cells progressively increased in regenerating tips (Fig. 6A-C), including BrdU$^+$/*cnox-2*$^+$ cells surrounding the newly formed mouth opening (Fig. 6B,C). Interestingly most *cnox-2*$^+$ cells were BrdU$^+$, corresponding to pairs of i-cells (Fig. 6D,F) and differentiated neurons (Fig. 6E). These pairs of i-cells, either asymmetric (Fig. 6D) or symmetric (Fig. 6F), frequently exhibited elongated processes, indicating that neuronal differentiation was taking place, resulting in mature neurons that were rare at 20 hpa but frequent at 44 hpa, still exhibiting some BrdU labeling. In a few BrdU$^+$ pairs of differentiating neurons, one of the two cells did not express *cnox-2* (not shown). These data indicate that the *cnox-2*$^+$ neurons detected at the early-late phase of head regeneration result from a differentiation process of *cnox-2*$^+$ neuronal precursors, rather than induction of *cnox-2* expression in mature neurons that would migrate and express *cnox-2* once they have reached the regenerating tip.

The blockade in head regeneration in the nerve-free *sf-1* mutant correlates with the lack of *cnox-2* expression

sf-1 hydra maintained at a permissive temperature regenerated their head efficiently, although delayed by 60 hours when compared with wild-type hydra (Fig. 7A). At a restrictive temperature, regeneration

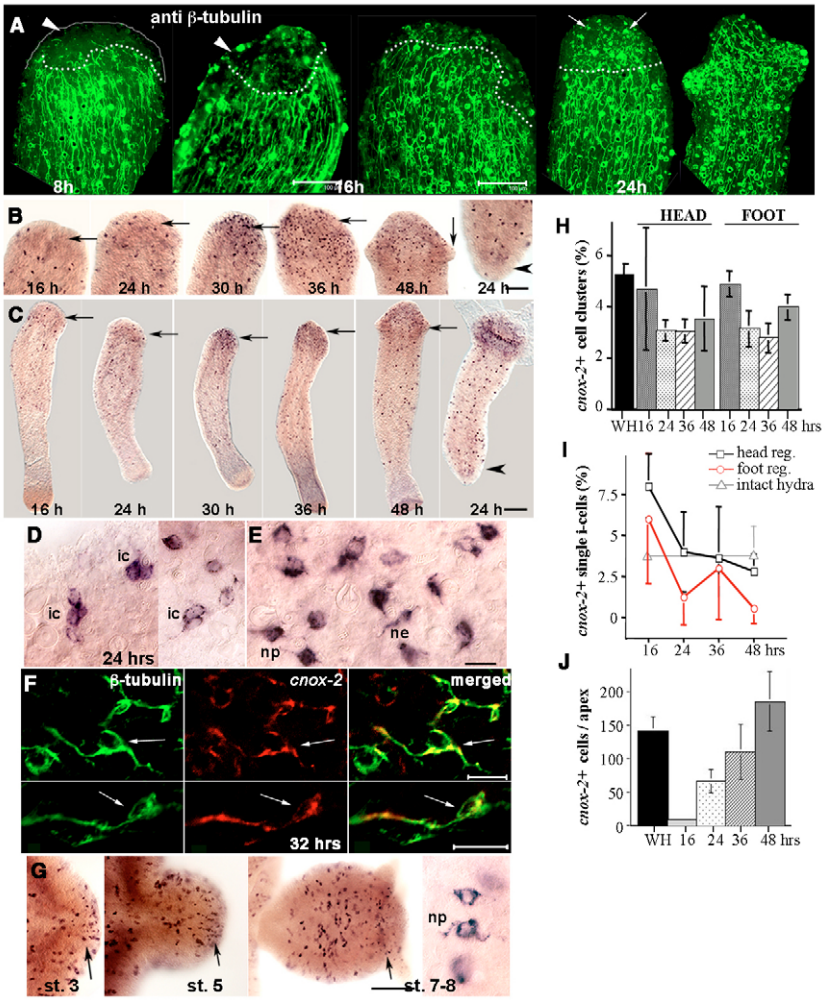

Fig. 5. Concomittant de novo neurogenesis and *cnox-2* expression at the early-late stage of head regeneration. (**A**) Anti-β-tubulin immunostaining of the nervous system in head-regenerating halves (see also Fig. S3 in the supplementary material). Neuronal processes are absent from the tips (arrowhead, boundary indicated with dots) up to 32 hpa when neuronal precursors differentiate (arrows). (**B-G**) *cnox-2* expression in the presumptive head region (arrows) detected about 20 hours before TBs emerge during both head regeneration at 24 hpa (B,D), and budding at stage 3 (G, arrows). (B) Enlarged views of the head- (arrows) and foot- (arrowhead) regenerating tips depicted in C. Note the absence of *cnox-2*$^+$ cells in the 16 hpa head-regenerating tip. (D-G) *cnox-2*$^+$ cells appear first as pairs of dividing i-cells (D), subsequently as neuronal percursors (E,G) and finally as differentiated neurons (arrows in F) in regenerating tips (D-F) and distal buds (G). (**H-J**) Transient variations in the *cnox-2*$^+$ cell distribution in regenerating halves (percentages calculated over DAPI-stained ectodermal cells). (H) Decrease in the gastric *cnox-2*$^+$ cell number. (I) Increase in *cnox-2*$^+$ single i-cells at 16 hpa. (J) Early-late increase in *cnox-2*$^+$ cells in head-regenerating tips. Scale bars: 200 μm in C; 100 μm in A,B,G; 20 μm in D,E,G right panel; 10 μm in F. ic, i-cell; ne, neuron; np, neuronal precursor.

was poorly efficient, as 45% hydra had not regenerated their head after 6 days and subsequently died (Fig. 7A). To test a possible correlation between the level of *cnox-2* expression and the efficiency of the head regeneration process, hydra were collected at different time points and sorted out according to both their *cnox-2*$^+$ apical cell number (null, low: fewer than 20, normal: more than 20) and their phenotype (Fig. 7B). The phenotypes were identified as Stage 1, 'ball-shape' with no obvious apical pole; Stage 2, 'elongated' with clearly distinguishable basal and apical poles; Stage 3, 'TB1' when the TBs have just emerged; Stage 4, 'TB2' when more than two TBs elongate; Stage 5, 'fully head-regenerated', similar to the adult head (Fig. 7C-H).

The ball-shaped hydra (n=22) never showed any *cnox-2* expression (Fig. 7C); this was also the case for most elongated hydra (75%, n=17, Fig. 7D), the others displaying a few *cnox-2*$^+$ cells (not shown). By contrast, most TB1 hydra exhibited a few *cnox-2*$^+$ cells (82%, Fig. 7E, arrows, n=16), the others (18%) being null for *cnox-2*. Among the latter, some probably underwent an 'aborted' regeneration process, as evidenced by their abnormal shape and the presence of a single tentacle bud (Fig. 7G,H, arrowheads). The emergence of a single tentacle was never observed in control hydra. At Stage 4 (n=31) and Stage 5 (n=14), 45 and 57% hydra displayed a normal number of *cnox-2*$^+$ cells, respectively (Fig. 7F); nevertheless a significant number of hydra exhibited no (16 and 7%) or low (39 and 29%) *cnox-2* expression. We also noted some sporadic gastric single *cnox-2*$^+$ cells but never observed *cnox-2*$^+$ cell clusters.

By contrast, the *cnox-2* expression pattern in regenerating *sf-1* hydra maintained at a permissive temperature was similar to that recorded in wild-type hydra: numerous *cnox-2* apical cells at the elongated shape stage (Fig. 7I) and a dense *cnox-2*$^+$ neuronal network at later stages (Fig. 7J,K). Along the body column, *cnox-2*$^+$ cell clusters became visible first in the aboral region (Fig. 7I) and then homogenously distributed along the axis (Fig. 7K). These data suggest a correlation between the level of *cnox-2* apical expression and the efficiency of the head-regeneration process, even though in a few cases (7%), a complete head regeneration process occurred when *cnox-2* expression was lacking or only transient.

Knocking down *cnox-2* expression prevents de novo neurogenesis and apical patterning during head regeneration

To test the *cnox-2* function during head regeneration, hydra were exposed to dsRNAs repeatedly and bisected. Emergence of TBs was delayed by 42 hours in those hydra when compared with controls and at 39 hpa, the ANS was not formed (Fig. 8A,I,J). The number of *cnox-2*$^+$ apical cells detected in head-regenerating tips of *Kazal1*(–) hydra increased over time in a similar way to non-treated hydra (Fig.

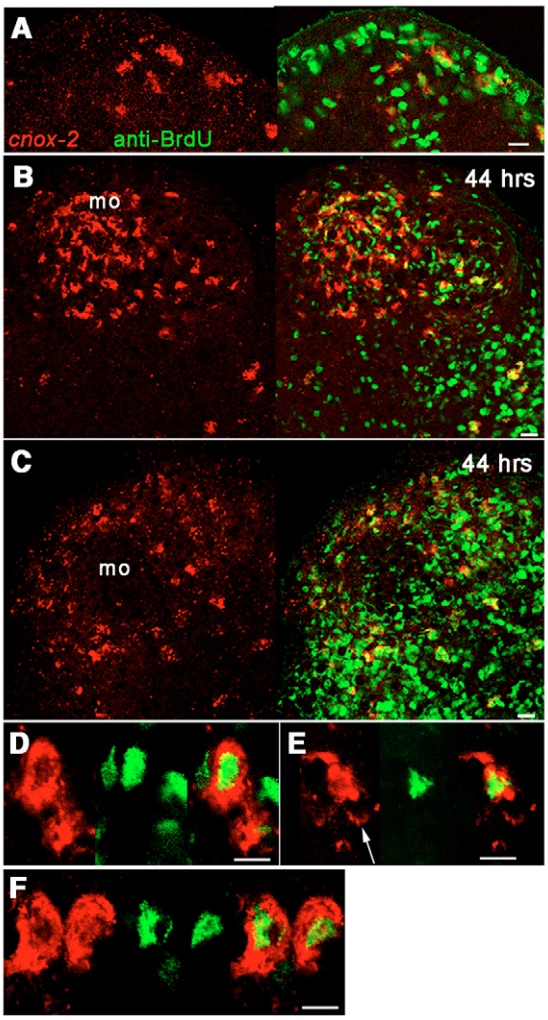

Fig. 6. *cnox-2*+ cells in head-regenerating tips that have just traversed the cell cycle. (**A-C**) Head-regenerating tips oriented toward the top, showing increasing density of BrdU-labeled (green) and *cnox-2*+ (red) cells, ultimately surrounding the mouth opening at 44 hpa (B,C). (**D-F**) Confocal views of BrdU$^+$/*cnox-2*$^+$ apical cells (green/red), which appear as asymmetrical pairs (D), differentiating processes (E, arrow) or dividing i-cells (F). Hydra (*Hv*), BrdU-labeled before amputation, were fixed at 20 hpa (A,D,E), 32 hpa (F) and 44 hpa (B,C). Scale bars: 10 μm. mo, mouth opening.

8B,D,F). By contrast, at 30 hpa twice as few *cnox-2*$^+$ apical cells were detected in *cnox-2*(–) hydra (Fig. 8E, arrow) as in *Kazal1*(–) or control hydra (55 and 53%, respectively, Fig. 8B). At 48 hpa, two distinct phenotypes were observed: strong (Fig. 8G) when the animal size was small, the regeneration stacked as evidenced by the absence of TBs (arrowheads in Fig. 8F) and the number of *cnox-2*$^+$ apical cells low (Fig. 8B); weak when the animal size was larger (although smaller than in *Kazal1*(–) hydra), the appearance of TBs only delayed (Fig. 8H, arrowhead) and the number of *cnox-2*$^+$ neurons closer to that observed in control hydra (35 per tip, Fig. 8B, black bar). Thus a clear correlation between the level of *cnox-2*$^+$ apical expression and the efficiency in de novo head formation was observed in *cnox-2* dsRNA-treated hydra.

Interestingly, when considering the number of gastric *cnox-2*$^+$ cell clusters, no correlation with the head-regeneration phenotype was evidenced. In fact, at 30 hpa, this number was similar in *Kazal1*(–) and *cnox-2* knockdown hydra. However, at 48 hpa, *cnox-2*(–) hydra had not yet reestablished *cnox-2* expression in their body column (Fig. 8C,G,H), by contrast to control and *Kazal1*(–) hydra (Fig. 8F).

DISCUSSION

The hydra *gsx* homolog *cnox-2* is a marker of bipotent neuronal progenitors

In this work we show that *cnox-2*$^+$ cells correspond to precursors as well as derivatives of two distinct cell lineages, taking into account their position along the body axis, their morphology and their clustered organization. These are: (1) a subset of neurons and their precursor cells in the apex; and (2) dividing i-cells as well as proliferating nematoblasts in the body column. This fate restriction of *cnox-2*$^+$ cells is supported by the complete and rapid disappearance of *cnox-2*$^+$ cells in *sf-1* mutants. Hence these two cell lineages, which are known to share a common interstitial stem cell (Bode, 1996), also share a common set of evolutionarily-conserved regulatory genes, which, in addition to the ParaHox *gsx/cnox-2* gene (this work), includes the *hyCOUP-TF* nuclear orphan receptor, the PRD-CLASS homeogene *prdl-b* (Gauchat et al., 2004) and the *Achaete-scute* homolog *CnASH* (Hayakawa et al., 2004). None of these four genes were found expressed in any other derivatives of the interstitial stem cells or in myoepithelial cells. Among the *hyCOUP-TF*$^+$ and *prdl-b*$^+$ cells, single i-cells were not observed and pairs of dividing i-cells were rare (Gauchat et al., 2004). Furthermore, *CnASH* is a marker for non-proliferating differentiating nematoblasts (Lindgens et al., 2004) and differentiating sensory neurons (Hayakawa et al., 2004). Therefore, *cnox-2* occupies a unique position among the putative regulators of the hydra nervous system, as it identifies a highly proliferative subset of i-cells, the progeny of which are restricted to neuronal and mechanosensory cell fates. Similarly, a subpopulation of i-cells was shown to be restricted to a gametic fate (Littefield, 1991; Nishimiya-Fujisawa and Sugiyama, 1993), but this is the first report concerning the somatic lineages. Previous studies showed that neuronal precursors from the peduncle could actually provide nematocyte precursors after transplantation into a gastric environment (Holstein and David, 1990b), suggesting that these two cell lineages indeed share common specific precursors. In the absence of one of the criteria that define stem cells, i.e. the evidence that these cells can self-renew (Weissman et al., 2001), we propose to consider the *cnox-2*$^+$ i-cells as progenitors to neurons and mechanosensory cells (Fig. 4C). Interestingly, in mice, the *gsx* homologs *Gsh1* and *Gsh2* appear to control the size and the identity of neuronal progenitor pools (Toresson and Campbell, 2001; Yun et al., 2003).

cnox-2 is an upstream regulator of neurogenesis and nematocyte differentiation

Although genes expressed in neurons are readily refractory to RNAi (Tavernarakis et al., 2000), the feeding RNAi strategy we applied for the first time in hydra to silence a neurally expressed gene, indeed induced specific effects, including a drastic disorganization of the ANS and a deficient head-regeneration process. In both contexts, intact or regenerating hydra, the number of *cnox-2*$^+$ cells (i-cells, apical neurons, nematoblasts) was significantly reduced after repeated exposures to *cnox-2* dsRNA. Moreover, the *prdl-a*, *gsc*, *RFamide-B* and *RFamide-C* that are specifically expressed in apical neurons, were strongly downregulated. Interestingly, the role of *cnox-2* in neurogenesis also probably extends to the body column, as the expression of the non-apical neuronal gene *msh* was altered in *cnox-2*(–) hydra. However, in the body column, we did not identify *cnox-2*+ neurons, suggesting that in this region *cnox-2*

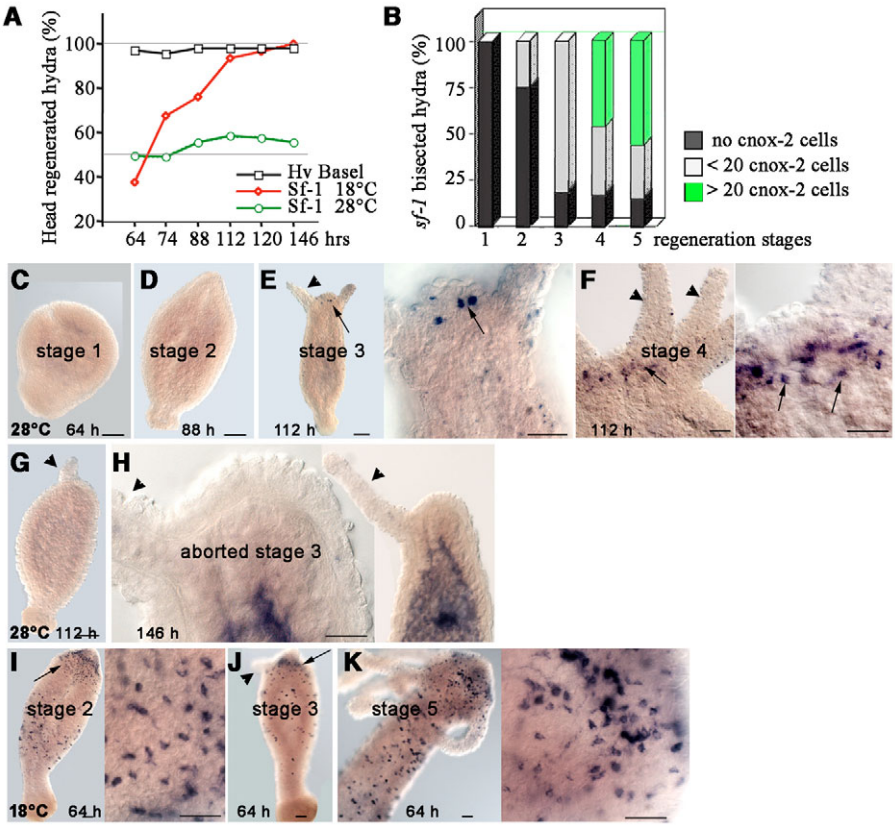

Fig. 7. Correlation between the *cnox-2*+ cell number in head-regenerating *sf-1* mutants and the regeneration phenotype. (**A**) Kinetics of head regeneration as assessed by TB emergence in wild-type hydra (black squares), *sf-1* hydra maintained at 18°C (red diamonds) or 28°C (green circles). (**B**) Number of *cnox-2*$^{+}$ apical cells in amputated *sf-1* hydra maintained at 28°C and sorted according to their regeneration stage (n=22, 17, 16, 31, 14). (**C-K**) *cnox-2* expression in amputated *sf-1* hydra maintained at 28°C (C-H) or 18°C (I-K). (C) ball-shape stage-1; (D,I) elongated stage-2; (E,G,H,J) TB1 stage-3; (F) TB2 stage-4; (K) fully-regenerated stage-5. Endodermal staining is artefactual as samples were overstained. Scale bars: 100 μm.

function is restricted to neuronal progenitors, whereas in the apex *cnox-2* would be required at least at two distinct levels, to commit interstitial cells to the neuronal fate and to promote the differentiation of multipolar neurons.

The striking genetic regulations observed in *cnox-2*(–) hydra also indicate possible epistatic relationships in the nematocyte pathway (Fig. 4C). *cnox-2* appears as one of the earliest activated genes and possibly regulates the commitment of i-cells to the nematocyte pathway as well as the proliferation of nematoblasts, turning on *hyZic*, directly or indirectly. By contrast, *cnox-2* and/or *hyZic* probably negatively regulate *hyCOUP-TF* in proliferating nematoblasts, because *hyCOUP-TF* is supposed to act as a repressor of proliferation (Gauchat et al., 2004) and is upregulated in *cnox-2*(–) hydra. As previously proposed, *hyZic* might regulate *CnASH* positively in differentiating nematocytes (Lindgens et al., 2004). At least two genes expressed in this pathway were not affected: *CREB* and *NOWA*, a structural gene involved in nematocyst differentiation (Engel et al., 2002). *CREB* could act upstream of *cnox-2* in this cell lineage. However, as CREB is strongly expressed in i-cells, proliferating nematoblasts, differentiated neurons and myoepithelial cell lineages (Kaloulis et al., 2004; Chera et al., 2007), its regulation within a specific cell lineage cannot be uncovered in RT-PCR assays and requires further analyses. Finally the stable low level of *NOWA* transcripts suggests that a longer period of *cnox-2* silencing might be required before differentiated nematocytes are affected.

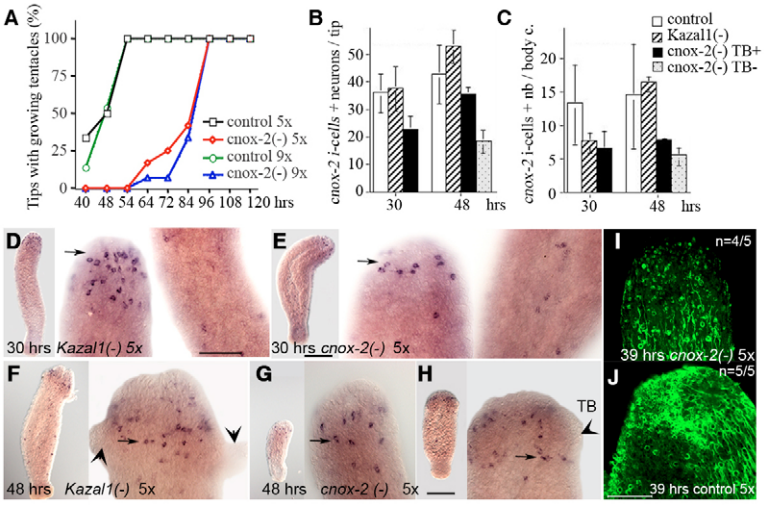

Fig. 8. Head regeneration is altered in *cnox-2* RNAi hydra. (**A**) Delay in head regeneration after 5× (n=12) and 9× (n=15) *cnox-2* dsRNA exposures. (**B-J**) Cellular analyses of head-regenerating hydra amputated after 5× exposures to dsRNAs. (B,C) Decrease in the number of *cnox-2*$^{+}$ cells in head-regenerating tips (B) and body column (C) of lower halves at 30 and 48 hpa. (D-H) *cnox-2* expression in head-regenerating hydra exposed to *Kazal1* (D,F) or *cnox-2* (E,G,H) dsRNAs. Right panels: enlarged views of tips (arrows), TBs (arrowheads) and body column (D,E). Note the small size and the delayed regeneration of animals shown in G,H when compared with F. (I,J) Anti-β-tubulin staining of head-regenerating tips at 39 hpa in hydra exposed to *cnox-2* (I) or control (J) dsRNAs. Results depicted in panels A,B-H,I,J correspond to three independent experiments. Scale bars: 200 μm in D-H; 100 μm in I,J.

cnox-2, a marker for de novo neurogenesis at the early-late stage of head regeneration

Genes expressed within the head-regenerating tips exhibit modulations that are temporally characterized as 'immediate', 'early', 'early-late' and 'late', matching with the wound healing, the setting up of the organizer activity, the proliferation phase or following head formation, respectively (Galliot and Schmid, 2002). As *cnox-2* expression in the presumptive head region resumes after 16 hpa, *cnox-2* belongs to the 'early-late' genes. Previous hydroxurea experiments showed that cells in S-phase at the time of amputation provide newly differentiated neurons in head-regenerating tips (Venugopal and David, 1981; Holstein et al., 1986). The analysis of the BrdU$^+$/*cnox-2*$^+$ cells confirms this result: i-cells in S-phase at amputation time undergo mitosis and neuronal differentiation 20 to 30 hours later in head-regenerating tips. As those tips contain very few BrdU$^+$ cells immediately after amputation (Holstein et al., 1991) (S.C. and L.G., unpublished), we anticipate that those cells first migrate toward the tip and become *cnox-2*$^+$ upon exposure to head-specific differentiation signal(s). This scenario fits with the injury effects previously described: injury promotes the migration of i-cells (Fujisawa et al., 1990), which is enhanced by the signals released by the head-regenerating tips (Teragawa and Bode, 1991). Those signals also drive the terminal differentiation of neuronal precursors within about 18 hours (Venugopal and David, 1981; Holstein et al., 1986). Hence, *cnox-2* appears to be a target gene for neurogenic signals during head formation. A similar continuous phenotypic maturation of neurons occurs from the gastric region to the basal extremity, accelerated upon amputation (Technau and Holstein, 1996), suggesting that de novo neurogenesis rather than phenotypic conversion of existing neurons (Bode, 1992) is the predominant mechanism during regeneration.

i-cell proliferation and de novo apical neurogenesis support head patterning in wild-type hydra

In two distinct contexts in which *cnox-2* expression was reduced or undetectable, i.e. RNAi-silenced wild-type hydra and *sf-1* mutants, head regeneration was dramatically altered. As *cnox-2* supports proliferation of i-cells and de novo neurogenesis at the early-late stage, these results support the importance of these two cellular processes in head-regenerating tips for head patterning, and the possible contribution of neuronal cells as previously proposed (Schaller et al., 1989).

Nevertheless, in a few *sf-1* hydra in which the number of *cnox-2*$^+$ cells was low or null, the head regeneration process was advanced or complete. We anticipate that such animals maintained for several days at restrictive temperature might have transiently expressed *cnox-2*, allowing the head formation process to proceed, subsequently losing *cnox-2* expression and/or *cnox-2*$^+$ cells. Alternatively a nerve-independent regeneration process might have taken over in these animals. Similarly, in *cnox-2*(–) hydra that had ultimately regenerated their head, either *cnox-2* silencing was transient and *cnox-2* expression reestablished at the time of head formation, or a *cnox-2*-independent alternative mechanism was activated. Recently, a similar correlation between the disappearance of *Dickkopf*+ gland cells and the blockade in head regeneration in *sf-1* hydra was reported (Guder et al., 2006), suggesting that gland cells, besides their immediate cytoprotective effect (Chera et al., 2006), also participate in the head regeneration process.

The nerve-dependence of regeneration across evolution

Comparative analysis of the regeneration processes in urodeles and hydra imposed opposed views concerning their respective nerve-dependence: in urodeles nerve-dependence is complete, as neurotrophic factors are required for the proliferation of blastema cells (Singer, 1974), whereas in hydra, nerve-dependence is dispensable, as nerve-free animals regenerate (Marcum and Campbell, 1978; Sugiyama and Fujisawa, 1978). However, in urodeles the nerve-dependence is linked to the preexisting homeostatic conditions, as limbs that developed in the absence of nerves (aneurogenic limbs) are able to regenerate in the absence of any neuronal support (Brockes, 1987; Tassava and Olsen-Winner, 2003), mimicking the nerve-free hydra situation. In such hydra, the genetic program at work in epithelial cells is not yet known, but is likely to be different from that at work in wild-type hydra (Schaller et al., 1980; Hornberger and Hassel, 1997) (S.C., unpublished). In the head-regeneration deficient mutant *reg-16*, removal of i-cells rescues head regeneration, highlighting the morphogenetic consequences of a misregulation between i-cells and myoepithelial cells (Sugiyama and Wanek, 1993). We propose that in the wild-type context, at the stage of head formation, hydra makes use of cell proliferation and de novo neurogenesis, both requiring cnox-2 activity. This sequence of events would be the most efficient and the fastest way to achieve head regeneration. In the absence of one of these components, i-cell proliferation, neuronal differentiation and *cnox-2* activation, other routes can be taken, although much slower and much less efficient.

We thank Virginie Voeffray and Fabienne Chabaud for excellent technical help, Corina Guder and Thomas Holstein for providing the *sf-1* hydra, Alejandro Sanchez-Alvarado and Jeremy Brockes for helpful discussions, and Ariel Ruiz-i-Altaba and Volker Schmid for precious comments on this manuscript. This work was supported by the Swiss National Foundation, the Geneva Canton, the Fonds Claraz and the Geneva Academic Society.

Supplementary material

Supplementary material for this article is available at http://dev.biologists.org/cgi/content/full/134/6/1191/DC1

References

Bode, H. R. (1992). Continuous conversion of neuron phenotype in hydra. *Trends Genet.* **8**, 279-284.

Bode, H. R. (1996). The interstitial cell lineage of hydra: a stem cell system that arose early in evolution. *J. Cell Sci.* **109**, 1155-1164.

Bosch, T. C. and David, C. N. (1984). Growth regulation in Hydra: relationship between epithelial cell cycle length and growth rate. *Dev. Biol.* **104**, 161-171.

Brockes, J. P. (1987). The nerve dependence of amphibian limb regeneration. *J. Exp. Biol.* **132**, 79-91.

Broun, M., Sokol, S. and Bode, H. R. (1999). Cngsc, a homologue of goosecoid, participates in the patterning of the head, and is expressed in the organizer region of Hydra. *Development* **126**, 5245-5254.

Campbell, R. D. and David, C. N. (1974). Cell cycle kinetics and development of Hydra attenuata. II. Interstitial cells. *J. Cell Sci.* **16**, 349-358.

Cartwright, P., Bowsher, J. and Buss, L. W. (1999). Expression of a Hox gene, Cnox-2, and the division of labor in a colonial hydroid. *Proc. Natl. Acad. Sci. USA* **96**, 2183-2186.

Chera, S., de Rosa, R., Miljkovic-Licina, M., Dobretz, K., Ghila, L., Kaloulis, K. and Galliot, B. (2006). Silencing of the hydra serine protease inhibitor Kazal1 gene mimics the human Spink1 pancreatic phenotype. *J. Cell Sci.* **119**, 846-857.

Chera, S., Kaloulis, K. and Galliot, B. (2007). The cAMP Response Element Binding Protein (CREB) as an integrative HUB selector in metazoans: clues from the hydra model system. *Biosystems* **87**, 191-203.

Engel, U., Ozbek, S., Streitwolf-Engel, R., Petri, B., Lottspeich, F., Holstein, T. W., Oezbek, S. and Engel, R. (2002). Nowa, a novel protein with minicollagen Cys-rich domains, is involved in nematocyst formation in Hydra. *J. Cell Sci.* **115**, 3923-3934.

Finnerty, J. R., Paulson, D., Burton, P., Pang, K. and Martindale, M. Q. (2003). Early evolution of a homeobox gene: the parahox gene Gsx in the Cnidaria and the Bilateria. *Evol. Dev.* **5**, 331-345.

Fujisawa, T. (1989). Role of interstitial cell migration in generating position-dependent patterns of nerve cell differentiation in Hydra. *Dev. Biol.* **133**, 77-82.
Fujisawa, T. (2003). Hydra regeneration and epitheliopeptides. *Dev. Dyn.* **226**, 182-189.
Fujisawa, T. and Sugiyama, T. (1978). Genetic analysis of developmental mechanisms in Hydra. IV. Characterization of a nematocyst-deficient strain. *J. Cell Sci.* **30**, 175-185.
Fujisawa, T. and David, C. N. (1984). Loss of differentiating nematocytes induced by regeneration and wound healing in Hydra. *J. Cell Sci.* **68**, 243-255.
Fujisawa, T., David, C. N. and Bosch, T. C. (1990). Transplantation stimulates interstitial cell migration in hydra. *Dev. Biol.* **138**, 509-512.
Galliot, B. and Miller, D. (2000). Origin of anterior patterning. How old is our head? *Trends Genet.* **16**, 1-5.
Galliot, B. and Schmid, V. (2002). Cnidarians as a model system for understanding evolution and regeneration. *Int. J. Dev. Biol.* **46**, 39-48.
Galliot, B., Miljkovic-Licina, M. and Chera, S. (2006). Hydra: a niche for cell and developmental plasticity. *Semin. Cell Dev. Biol.* **17**, 492-502.
Gauchat, D., Kreger, S., Holstein, T. and Galliot, B. (1998). prdl-a, a gene marker for hydra apical differentiation related to triploblastic paired-like head-specific genes. *Development* **125**, 1637-1645.
Gauchat, D., Mazet, F., Berney, C., Schummer, M., Kreger, S., Pawlowski, J. and Galliot, B. (2000). Evolution of Antp-class genes and differential expression of Hydra Hox/paraHox genes in anterior patterning. *Proc. Natl. Acad. Sci. USA* **97**, 4493-4498.
Gauchat, D., Escriva, H., Miljkovic-Licina, M., Chera, S., Langlois, M. C., Begue, A., Laudet, V. and Galliot, B. (2004). The orphan COUP-TF nuclear receptors are markers for neurogenesis from cnidarians to vertebrates. *Dev. Biol.* **275**, 104-123.
Guder, C., Pinho, S., Nacak, T. G., Schmidt, H. A., Hobmayer, B., Niehrs, C. and Holstein, T. W. (2006). An ancient Wnt-Dickkopf antagonism in Hydra. *Development* **133**, 901-911.
Hayakawa, E., Fujisawa, C. and Fujisawa, T. (2004). Involvement of Hydra achaete-scute gene CnASH in the differentiation pathway of sensory neurons in the tentacles. *Dev. Genes Evol.* **214**, 486-492.
Hayward, D. C., Catmull, J., Reece-Hoyes, J. S., Berghammer, H., Dodd, H., Hann, S. J., Miller, D. J. and Ball, E. E. (2001). Gene structure and larval expression of cnox-2Am from the coral Acropora millepora. *Dev. Genes Evol.* **211**, 10-19.
Holstein, T. W. and David, C. N. (1990a). Cell cycle length, cell size, and proliferation rate in hydra stem cells. *Dev. Biol.* **142**, 392-400.
Holstein, T. W. and David, C. N. (1990b). Putative intermediates in the nerve cell differentiation pathway in hydra have properties of multipotent stem cells. *Dev. Biol.* **142**, 401-405.
Holstein, T., Schaller, C. H. and David, C. N. (1986). Nerve cell differentiation in Hydra requires two signals. *Dev. Biol.* **115**, 9-17.
Holstein, T. W., Hobmayer, E. and David, C. N. (1991). Pattern of epithelial cell cycling in hydra. *Dev. Biol.* **148**, 602-611.
Holstein, T. W., Hobmayer, E. and Technau, U. (2003). Cnidarians: an evolutionarily conserved model system for regeneration? *Dev. Dyn.* **226**, 257-267.
Hornberger, M. R. and Hassel, M. (1997). Expression of HvRACK1, a member of the RACK1 subfamily of regulatory WD40 proteins in Hydra vulgaris, is coordinated between epithelial and interstitial cells in a position-dependent manner. *Dev. Genes Evol.* **206**, 435-446.
Javois, L. C. and Frazier-Edwards, A. M. (1991). Simultaneous effects of head activator on the dynamics of apical and basal regeneration in Hydra vulgaris (formerly Hydra attenuata). *Dev. Biol.* **144**, 78-85.
Kaloulis, K., Chera, S., Hassel, M., Gauchat, D. and Galliot, B. (2004). Reactivation of developmental programs: The cAMP-response element-binding protein pathway is involved in hydra head regeneration. *Proc. Natl. Acad. Sci. USA* **101**, 2363-2368.
Lindgens, D., Holstein, T. W. and Technau, U. (2004). Hyzic, the Hydra homolog of the zic/odd-paired gene, is involved in the early specification of the sensory nematocytes. *Development* **131**, 191-201.
Littefield, C. L. (1991). Cell lineages in Hydra: isolation and characterization of an interstitial stem cell restricted to egg production in Hydra oligactis. *Dev. Biol.* **143**, 378-388.
MacWilliams, H. K. (1983). Hydra transplantation phenomena and the mechanism of Hydra head regeneration. II. Properties of the head activation. *Dev. Biol.* **96**, 239-257.
Marcum, B. A. and Campbell, R. D. (1978). Development of Hydra lacking nerve and interstitial cells. *J. Cell Sci.* **29**, 17-33.
Marcum, B. A., Fujisawa, T. and Sugiyama, T. (1980). A mutant hydra strain (sf-1) containing temperature-sensitive interstitial cells. In *Developmental and Cellular Biology of Coelenterates* (ed. P. Tardent and R. Tardent), pp. 429-434. Amsterdam: Elsevier/North Holland.
Miljkovic-Licina, M., Gauchat, D. and Galliot, B. (2004). Neuronal evolution: analysis of regulatory genes in a first-evolved nervous system, the hydra nervous system. *Biosystems* **76**, 75-87.
Mitgutsch, C., Hauser, F. and Grimmelikhuijzen, C. J. (1999). Expression and developmental regulation of the Hydra-RFamide and Hydra- LWamide preprohormone genes in Hydra: evidence for transient phases of head formation. *Dev. Biol.* **207**, 189-203.
Nishimiya-Fujisawa, C. and Sugiyama, T. (1993). Genetic analysis of developmental mechanisms in hydra. XX. Cloning of interstitial stem cells restricted to the sperm differentiation pathway in Hydra magnipapillata. *Dev. Biol.* **157**, 1-9.
Otto, J. J. and Campbell, R. D. (1977). Budding in Hydra attenuata: bud stages and fate map. *J. Exp. Zool.* **200**, 417-428.
Schaller, H. C., Rau, T. and Bode, H. (1980). Epithelial cells in nerve-free hydra produce morphogenetic substances. *Nature* **283**, 589-591.
Schaller, H. C., Hoffmeister, S. A. and Dubel, S. (1989). Role of the neuropeptide head activator for growth and development in hydra and mammals. *Development* **107**, 99-107.
Schierwater, B., Dellaporta, S. and DeSalle, R. (2002). Is the evolution of Cnox-2 Hox/ParaHox genes "multicolored" and "polygenealogical?" *Mol. Phylogenet. Evol.* **24**, 374-378.
Schummer, M., Scheurlen, I., Schaller, C. and Galliot, B. (1992). HOM/HOX homeobox genes are present in hydra (Chlorohydra viridissima) and are differentially expressed during regeneration. *EMBO J.* **11**, 1815-1823.
Seipel, K. and Schmid, V. (2005). Evolution of striated muscle: jellyfish and the origin of triploblasty. *Dev. Biol.* **282**, 14-26.
Shenk, M. A., Bode, H. R. and Steele, R. E. (1993a). Expression of Cnox-2, a HOM/HOX homeobox gene in hydra, is correlated with axial pattern formation. *Development* **117**, 657-667.
Shenk, M. A., Gee, L., Steele, R. E. and Bode, H. R. (1993b). Expression of Cnox-2, a HOM/HOX gene, is suppressed during head formation in hydra. *Dev. Biol.* **160**, 108-118.
Siddiqui, S. S., Aamodt, E., Rastinejad, F. and Culotti, J. (1989). Anti-tubulin monoclonal antibodies that bind to specific neurons in Caenorhabditis elegans. *J. Neurosci.* **9**, 2963-2972.
Singer, M. (1974). Neurotrophic control of limb regeneration in the newt. *Ann. N.Y. Acad. Sci.* **228**, 308-322.
Sugiyama, T. and Fujisawa, T. (1978). Genetic analysis of developmental mechanisms in Hydra. II. Isolation and characterization of an interstitial cell-deficient strain. *J. Cell Sci.* **29**, 35-52.
Sugiyama, T. and Wanek, N. (1993). Genetic analysis of developmental mechanisms in hydra. XXI. Enhancement of regeneration in a regeneration-deficient mutant strain by the elimination of the interstitial cell lineage. *Dev. Biol.* **160**, 64-72.
Tassava, R. A. and Olsen-Winner, C. L. (2003). Responses to amputation of denervated ambystoma limbs containing aneurogenic limb grafts. *J. Exp. Zoolog. A Comp. Exp. Biol.* **297**, 64-79.
Tavernarakis, N., Wang, S. L., Dorovkov, M., Ryazanov, A. and Driscoll, M. (2000). Heritable and inducible genetic interference by double-stranded RNA encoded by transgenes. *Nat. Genet.* **24**, 180-183.
Technau, U. and Holstein, T. W. (1996). Phenotypic maturation of neurons and continuous precursor migration in the formation of the peduncle nerve net in Hydra. *Dev. Biol.* **177**, 599-615.
Teragawa, C. K. and Bode, H. R. (1991). A head signal influences apical migration of interstitial cells in Hydra vulgaris. *Dev. Biol.* **147**, 293-302.
Timmons, L. and Fire, A. (1998). Specific interference by ingested dsRNA. *Nature* **395**, 854.
Toresson, H. and Campbell, K. (2001). A role for Gsh1 in the developing striatum and olfactory bulb of Gsh2 mutant mice. *Development* **128**, 4769-4780.
Venugopal, G. and David, C. N. (1981). Nerve commitment in Hydra. I. Role of morphogenetic signals. *Dev. Biol.* **83**, 353-360.
Weissman, I. L., Anderson, D. J. and Gage, F. (2001). Stem and progenitor cells: origins, phenotypes, lineage commitments, and transdifferentiations. *Annu. Rev. Cell Dev. Biol.* **17**, 387-403.
Westfall, J. A. (1996). Ultrastructure of synapses in the first-evolved nervous systems. *J. Neurocytol.* **25**, 735-746.
Yanze, N., Spring, J., Schmidli, C. and Schmid, V. (2001). Conservation of Hox/ParaHox-related genes in the early development of a cnidarian. *Dev. Biol.* **236**, 89-98.
Yun, K., Garel, S., Fischman, S. and Rubenstein, J. L. (2003). Patterning of the lateral ganglionic eminence by the Gsh1 and Gsh2 homeobox genes regulates striatal and olfactory bulb histogenesis and the growth of axons through the basal ganglia. *J. Comp. Neurol.* **461**, 151-165.